# CHAPTER 6

# ALL-DIELECTRIC METAMATERIALS BASED ON SPHERICAL AND CUBIC INCLUSIONS

Irina Vendik, Mikhail Odit, Dmitry Kozlov

*St. Petersburg Electrotechnical University, 5 Prof. Popov Str., St. Petersburg, 197376, Russia*

The 3D regular lattice of bi-spherical dielectric resonant inclusions arranged in a cubic lattice as two sets of spheres made from the same dielectric material having different radii and embedded in a host dielectric material with lower dielectric permittivity was carefully investigated. The magnetic resonance corresponding to the first Mie resonance in the spherical particles is achieved by forming a regular array of effective magnetic dipoles, and the structure of the identical spherical dielectric resonators can be designed as an isotropic μ–negative 3D-metamaterial. For the electric resonance it was found experimentally and by simulation that the resonant response of the electric dipole is weakly pronounced and the ε-negative behavior is remarkably suppressed. To enhance the electric dipole contribution we considered another kind of the symmetry of the bi-spherical arrangement of the particles corresponding to the face-centered cubic symmetry instead of the symmetry of NaCl analogue considered previously. Electromagnetic properties of a volumetric structure based on a regular lattice of identical cubic dielectric particles are also considered and analyzed as μ-negative metamaterial. The cubic particle based 3D-metamaterial is preferable for practical realization as compared with the spherical inclusions. For practical realization of all dielectric metamaterial the limitation of the dielectric permittivity of spherical inclusions should be taken into account. It is shown that to get double negative behavior of bi-spherical metamaterial, resonators with permittivity higher than 100 should be used. The same estimations could be made for rod, cylindrical resonators or any kind of dielectric resonators used as components for metamaterial design.

## 1. Introduction

Medium with simultaneously negative permittivity and permeability or so-called double negative medium (DNG) can be formed as a regular lattice of dielectric resonant inclusions. Metamaterials with desired values of permeability ±μ and permittivity ±ε have been developed by exciting electric and magnetic resonant modes. [1] Dielectric cubic, disk, cylindrical, or spherical resonators are suitable for establishing the dipole moments. For many practical cases, isotropic DNG structures are very attractive. Different ways to create a 3D isotropic DNG medium based on a regular lattice of resonant inclusions have been considered and published. [1-6] The 3D regular lattice of bi-spherical dielectric resonant inclusions was suggested in Ref. 2. In this structure, the metamaterial medium is composed of two sets of spherical particles made from the same dielectric material embedded in a host dielectric material. The spheres differ by radius. The dielectric constant of the spherical particles is much larger than that of the host material. By combining two sets of the spheres with suitable radii, different modes can be simultaneously excited in the spheres: the magnetic resonance mode giving rise to the magnetic dipole momentum and the electric resonance mode being responsible for the electric dipole momentum. The magnetic resonance corresponding to the first Mie resonance in the spherical particles is achieved by forming a regular array of effective magnetic dipoles, and the structure of the identical spherical dielectric resonators can be designed as an isotropic μ-negative 3D-metamaterial. The second Mie resonance is achieved by forming a regular array of effective electric dipoles, and the structure can be designed as an isotropic ε-negative 3D-metamaterial. These moments in the bi-spherical structure create the negative permeability and permittivity in a limited frequency range near the resonant frequency. In Refs. 3-5, it was suggested that the dielectric resonators do not interact and for the 3D structure the responses of both spherical particles are superimposed. By full-wave simulation and experimental investigation, it was found that the resonance response of the magnetic dipole is very effective and the μ-negative isotropic metamaterial can be designed as a regular array of dielectric spherical particles with the first Mie-resonance. At the same time, the electric

dipole corresponding to the electric resonance mode is weakly pronounced. As a consequence, the ε-negative behavior is blurred. [5]

Detailed theoretical description based on full-wave analysis was performed in Ref. 6 for different all-dielectric structures of metamaterial: single-negative (SNG) medium based on spherical particles; bi-spherical DNG medium based on an array of dielectric spherical particles of the same radius made from two materials differing in dielectric permittivity; a set of identical discs and discs made of two different dielectric materials etc. The structures based on the discs form 2D SNG and DNG metamaterials. The 2D structures based on cylindrical resonator arrays situated in a parallel-plate waveguide have been discussed and experimentally verified in Refs. 7-8. In these structures, the DNG properties are provided by magnetic resonance in the cylinders (magnetic dipole, μ-negative behavior) and by ε -negative response of electromagnetic wave in a parallel-plate metallic waveguide with $TE_n$ modes below the cut-off frequency [7] or by coupling between the cylindrical resonators. [8]

Recently the experimental investigations of isotropic metamaterials based on resonant dielectric inclusions have been reported. [9-11] The resonant μ-negative response was registered in the 3D structure based on a regular array of dielectric cubes [9] and in the 2D array of cubes. [10] The 3D DNG material was realized as a set of dielectric spherical particles regularly distributed in a metallic wire frame exhibiting cubic symmetry.[11] The wire frame provides an environment with evanescent waves followed by the effective negative permittivity, which is in combination with the resonant dielectric particles giving rise to magnetic dipoles and negative permeability.

All these achievements support the fruitful idea of a realization of an isotropic metamaterial using dielectric resonant inclusions. In order to improve the performance of the all dielectric DNG medium with cubic symmetry based on spherical dielectric particles, the changed symmetry of the single cell of the bi-spherical structure was suggested to enhance the contribution of the electric resonance in the effective dielectric permittivity. [12] The 3D DNG bi-spherical structure based on the single cell belonging to the body-centered cubic symmetry exhibits a higher packing density for the same distance between adjacent resonant

particles as compared with the face-centered cubic lattice previously analyzed in Refs. 2-5.

The regular lattice of strongly coupled dielectric resonant spherical particles also exhibits properties of the isotropic DNG medium. [13-14] In this regular array of identical dielectric spheres, the magnetic dipole is originated inside the spheres, whereas the electric dipole arises from the electrical coupling between the spheres.

Realization of the artificial DNG structure as a regular lattice of dielectric resonant inclusions is limited by parameters of the dielectric material: dielectric permittivity and loss factor. The dielectric permittivity is limited by the lower value and the loss factor is limited by the upper value. A specific approach to solve the problem of designing homogeneous DNG medium is suggested and discussed.

All the problems mentioned above are presented and discussed in this chapter.

## 2. Isotropic Bi-spherical Metamaterial of Cubic Symmetry with High Packing Density

Single cubic cells of isotropic metamaterial based on two types of spherical resonators having two different radii are presented in Fig 1. The dielectric constant of the spherical particles arranged in the host material

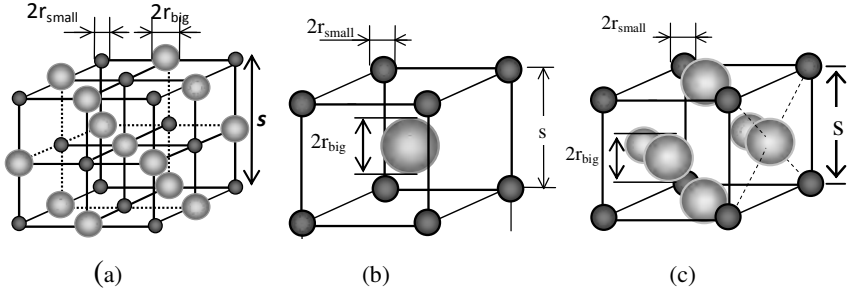


Fig. 1. (a) Face centered NaCl cell; (b) body-centered single cell; (c) face centered unit cell.

is much larger than that of the host material. By combining two sets of the spheres with suitable radii, two different modes $H_{111}$ and $E_{111}$ can be simultaneously excited in the spheres: the magnetic resonance mode

giving rise to the magnetic dipole momentum and the electric resonance mode being responsible for the electric dipole momentum. In Refs. 2-4, it was suggested that the dielectric resonators do not interact and for the 3D structure the responses of the both spherical particles are superimposed.

Different ways of particle packing are possible. The face-centered NaCl-like structure (Fig 1a), body-centered structure (Fig 1b) and other type of face-centered cubic lattice (Fig 1c) are all members of the cubic system of symmetry pertaining to the class *m3m* [3, 15]

In the case of cubic symmetry, the second rank tensors of all physical parameters of the media are diagonal and have the components of the same values. [15] Thus the permittivity and permeability tensors are written in the following form:

$$\varepsilon_{eff} = \begin{vmatrix} \varepsilon_{eff} & 0 & 0 \\ 0 & \varepsilon_{eff} & 0 \\ 0 & 0 & \varepsilon_{eff} \end{vmatrix}, \qquad \mu_{eff} = \begin{vmatrix} \mu_{eff} & 0 & 0 \\ 0 & \mu_{eff} & 0 \\ 0 & 0 & \mu_{eff} \end{vmatrix}, \tag{1}$$

where the sub-indices *eff* are introduced to stress that the permittivity and permeability are obtained as a result of averaging electric and magnetic polarization of spherical particles embedded in the matrix. The result of averaging the polarization of the spherical particles embedded in the matrix depends on the volume of the matrix falling on each particle considered. The medium with effective electromagnetic parameters is considered as a homogeneous one.

Body-centered and face-centered structures are related to the same class of symmetry and have the same form of the second rank tensor as the simple cubic structure. The structures considered are characterized by different distances between the particles of the same/different dimensions. These structures are characterized by a higher packing density as compared with the simple cubic structure.

The comparative Table 1 shows difference in these parameters for different packing factors for the same distance *a* between the particles situated on a shorter distance. The volume fraction for each structure is equal to the volume of sphere divided by the volume of single cell. The $v_f$ parameter is described by equation $v_f = 4/3 \cdot \pi r^3 / s^3$ (Fig. 2).

Simulations revealed that the particles should be placed as close as possible to each other in order to strengthen the DNG effect. At the same

time, a high density of the particles is followed by their mutual interaction and, as a consequence, shifting resonances and their distortion. That's why all the structures are considered with the same minimum distance between the closest resonators.

Table 1. Distances between particles for different structures.

| Structure | Lattice constant, s | Minimal distance between the large particles | Minimal distance between the small particles | Minimal distance between different particles | Volume fraction for the large particles | Volume fraction for the small particles |
|---|---|---|---|---|---|---|
| Face-centered (NaCl-like) | $2a$ | $s\sqrt{2}/2$ | $s\sqrt{2}/2$ | $s/2$ | $4v_f$ | $4v_f$ |
| Body-centered | $2a/\sqrt{3}$ | $s$ | $s$ | $s\sqrt{3}/2$ | $v_f$ | $v_f$ |
| Face-centered | $2a/\sqrt{2}$ | $s\sqrt{2}/2$ | $s$ | $s\sqrt{2}/2$ | $3v_f$ | $v_f$ |

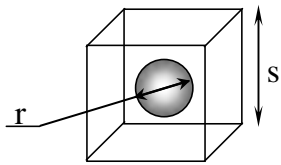


$$v_f = \frac{\frac{4}{3}\pi r^3}{s^3}$$

Fig. 2. Calculation of the volume fraction for a sphere in a single cell.

The electric dipole provided by the resonance in a larger sphere is weakly pronounced in comparison with the magnetic one. This could be explained by the electromagnetic field distribution inside spherical resonators. At the same time the value of the effective parameters depends on the volume fraction of the resonators. The higher volume fraction of the spheres – the higher will be the amplitude and bandwidth of the effective permeability or permittivity. This fact leads to the priority meaning of the density of the large resonators. In order to strength weak electric dipole one should increase volume fraction of the larger spheres.

Analyzing Table 1 we can conclude that the maximum volume fraction for the large resonators is observed for NaCl cell. At the same time, the concentration of large resonators in the face centered structure is 3 times higher, than in body-centered. This is valid in case the minimal distance between the closest particle is the same for all structures. Comparing NaCl and face-centered packing of the resonators one can see that the face-centered cell has smaller dimensions and a lower number of resonators whereas its volume fraction is $3v_f$ (in comparison with $4v_f$ for NaCl structure). Therefore the face centered structure is preferable from a practical point of view.

The effective electromagnetic parameters of the bi-spherical array have been analytically found by solving the problem of diffraction of the plane wave on the non-interacting dielectric spheres. [2-5, 13] For two different structures, the frequency dependent effective permittivity and permeability are calculated in the same way and determined as follows:

$$\varepsilon_r^{(eff)}(f) = F_{eps}\frac{1}{s^3}\varepsilon_p\frac{3}{2}I(f, r_{big})\cdot b^{(t)}(f, r_{big}) + \varepsilon_h, \tag{2}$$

$$\mu_r^{(eff)}(f) = F_{mu}\frac{1}{s^3}\sqrt{\frac{\varepsilon_p}{\varepsilon_h}}\frac{3}{2}I(f, r_{small})\cdot a^{(t)}(f, r_{small}) + \mu_h. \tag{3}$$

Here $s$ is the cell size (see Fig. 1), $\varepsilon_p$ ($\mu_p$), $\varepsilon_h$ ($\mu_h$) are the permittivity (permeability) of the particle and the host material respectively, $r_{small}$ and $r_{big}$ are the radii of the resonators, $f$ is the incident electromagnetic wave frequency, $a^{(t)}$ and $b^{(t)}$ are the amplitudes of spherical wave functions, $I$ is the result of integration of the electric and magnetic field components over the particle volume, [2-4], $F_{eps}$ and $F_{mu}$ depend on the type of structure: $F_{eps}$ = 0.5, 0.35, 0.65 and $F_{mu}$ = 0.5, 0.65, 0.65 for the NaCl-structure, body-centred and face-centred structures respectively.

In Fig. 3, the results of calculation of the effective parameters of the bi-spherical metamaterial are presented for two different structures with parameters: $\varepsilon_p$ = 400, $\varepsilon_h$ = 1, $\mu_p = \mu_h$ = 1, $r_{small}$ = 0.748 mm and $r_{big}$ = 1.05 mm. The loss factor of the dielectric material of the particles was taken $tan\delta$ = 0.0001. The host dielectric was assumed to be lossless. Evidently the response of the face-centered lattice is higher than that of the body-centered lattice. As a suitable dielectric material for the

resonant spherical inclusions, ceramics like BaO-SrO-$Nd_2O_3$-$TiO_2$ can be used; this material demonstrates $\varepsilon_r$ = 400 and tanδ ≤ 0.003 in the microwave region. [16, 17] In order to confirm the effectiveness of the face-centred lattice, let us consider the simplified case of one dimensional structure (Fig.4) using full-wave analysis. Due to the translation symmetry, the structure is bounded by perfect electric conductor (PEC) and perfect magnetic conductor (PMC). The structure contains 5 single cells along the wave propagation direction. The single cell is centered by the spherical particle of larger value of the radius $r_{big}$ ($r_{big}$ = 1.05 mm) and is surrounded by the particles of smaller value of the radius $r_{smal}$ ($r_{small}$ = 0.748 mm). The distance between the particles of the same size is s = 4 mm.

The particle dimensions are chosen to provide the magnetic resonance in the smaller spheres and the electric resonance in the larger

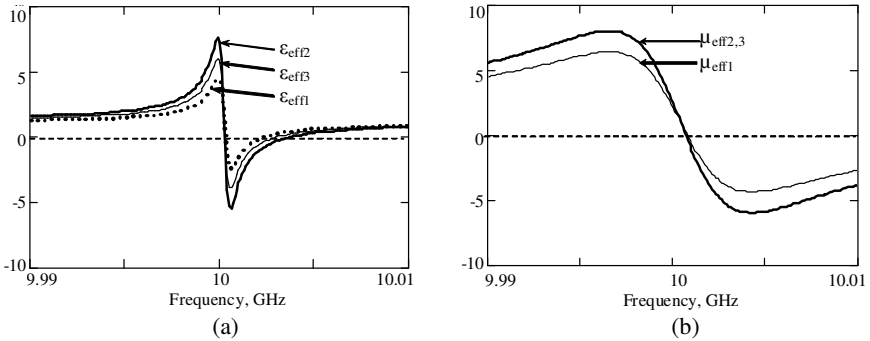


Fig. 3. Effective (a) permittivity and (b) permeability for face-centered Na-Cl structure (sub-index 1) the face-centered structure (sub-index 2) and body-centered structure (sub-index 3).

spherical particles at the same frequency. It results in creation of magnetic and electric dipoles followed by the negative effective permeability and effective permittivity in a limited frequency range. That leads to transmission of electromagnetic wave in this frequency range (Fig. 5). The full-wave analysis of the electromagnetic wave propagation confirms the existence of the backward wave.

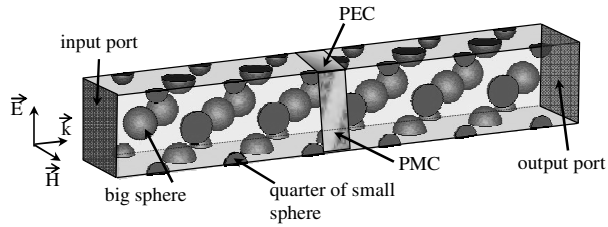


Fig. 4. 1-D structure of bi-spherical isotropic metamaterial. Radii of small and large spheres are 0.748 mm and 1.05 mm respectively. Boundary conditions are provided by perfect magnetic (PMC) and perfect electric (PEC) conductors.

The 3D volumetric structure is shown in Fig. 6. The small and big spherical particles are situated in different planes. The same is related to the magnetic and electric dipoles. The PECs and PMCs are used for providing boundary conditions for this limited in volume structure. The dimensions of the spherical particles and spacing between the identical particles are the same as in the previous case (Fig. 4). Magnetic field pattern for the section plane shown by yellow in Fig. 6 (a) is depicted in

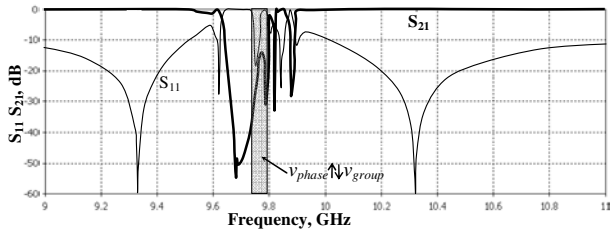


Fig. 5. Transmission S21 and reflection S11 coefficients for the structure depicted in Fig 4. Gray area is the frequency range, where the resonant frequencies of two types of resonances coincide and backward wave is observed.

Fig. 6 (b) for four different moments of the time period. Again the backward wave is observed. The response of the structure to the incident plane electromagnetic wave is presented in Fig. 7. In the limited frequency range one can observe the wave transmitting through the DNG structure.

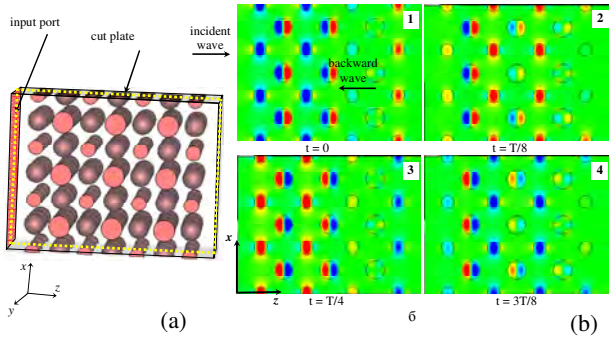


Fig. 6. (a) Bi-spherical structure of metamaterial with face-centered cubic symmetry. Radii of small and large spheres are 0.748 mm and 1.05 mm respectively. Distance between the same particles is 4 mm. (b) Magnetic field patterns for the section plane shown by yellow in (a) for 4 different moments of the period of time.

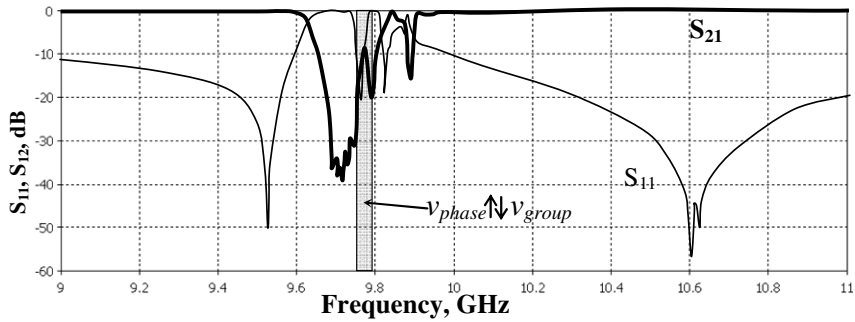


Fig. 7. Transmission $S_{21}$ and reflection $S_{11}$ coefficients for the structure depicted in Fig 6. Gray area is the frequency range where two types of resonances coincide and backward wave is observed.

## 3. 3D Metamaterial Based on Cubic Dielectric Resonant Inclusions

As it was shown, the 3D regular lattice based on resonant spherical inclusions exhibits properties of the DNG material. Unfortunately the practical realization of such a structure is very problematic.

To the best of our knowledge, there is just one publication demonstrating the experimental results of measuring transmission characteristic of the DNG medium based on the spherical inclusions inserted in the wire frame. [11] The experimental investigation of the 3D [9] and 2D [10] structures metamaterial-based on cubic resonant dielectric

inclusions confirmed the μ-negative properties of these artificial media. Modelling of electromagnetic characteristics of the lattice based on cubic dielectric inclusions was presented in Ref. 17. The regular 2D lattice of the dielectric cubes is shown in Fig. 8. The cubic particles are distantly positioned and the mutual coupling is negligibly small. In this case the frequency response of the structure is the same as for the material based on the identical spherical inclusions: the stop-band occurs near the resonant frequency, which corresponds to the μ-negative behaviour of the material.

The magnetic field distribution in the resonant particles for the first magnetic resonance in the spherical and cubic particles is shown in Fig. 9. Evidently the magnetic dipole in both cases is nearly the same. The results of full-wave simulation of the transmission through this structure consisting of two cubic layers are presented in Fig. 10. Transmission and reflection coefficients (Fig 10, (b)) exhibiting the stop-band near the resonant frequency.

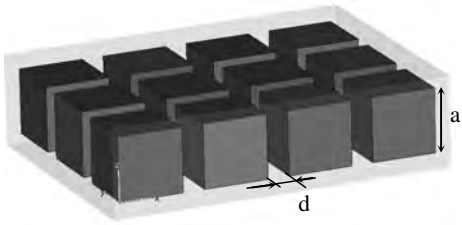


Fig. 8. The lattice of high permittivity dielectric cubes in the dielectric matrix of lower permittivity. The following parameters of cubes are used: size a = 3 mm, $\varepsilon_r$ = 1000, dielectric cube tan δ = 0.001, the distance between the cubes d = 1 mm.

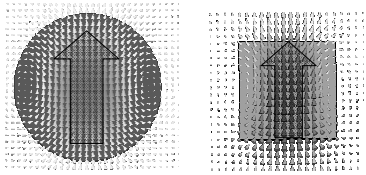


Fig. 9. Magnetic resonance in (a) the dielectric spherical particle (b) the dielectric cubic particle.

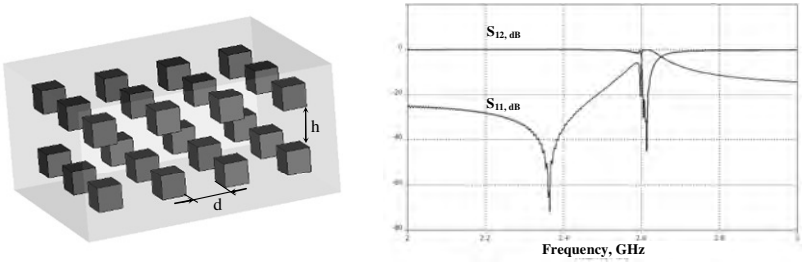


(a) (b)

Fig. 10. Two-layer dielectric cube structure (a). Transmission and reflection coefficients for the structure with the period $d$ = 5 mm and distance between the layers $h$ = 5 mm (b).

It was shown by simulation that for the structure with a finite number of the particles the resonant response depends on the number of layers: the more layers are used, the higher is the resonant frequency and the wider is the resonant response. That means that the coupling between the cubic particles influences the characteristics of the material.

The regular lattice of the cubic particles can be realized as a multilayer structure (for example multilayer structure based on Low-Temperature Cofired Ceramic, LTCC). In the general case, the 3D lattice can be designed being regular in plane with desired spacing between the layers. This spacing is determined by the ceramic layer thickness, whereas the lattice period in plane is determined by the mask dimensions. The results of modelling of the resonant characteristics of the structure based on the cubic dielectric resonators with the cube edge of 1 mm and the distance between the cubes of 3 mm in plane are shown in Fig. 11 for different numbers of the layers. The spacing between the layers is 1.2 mm. The resonant characteristics are split due to the strong coupling between the layers containing regular 2D lattice of the cubes.

The higher the number of layers containing the cubic resonant inclusions used, the more effective is the reflection from this artificial material. This can be used as an effective impedance surface without using any conducting or magnetic materials.

As in the case of bi-spherical structure, the bi-cubic lattice (Fig. 12, (a)) can be designed using magnetic and dielectric dipoles approach.

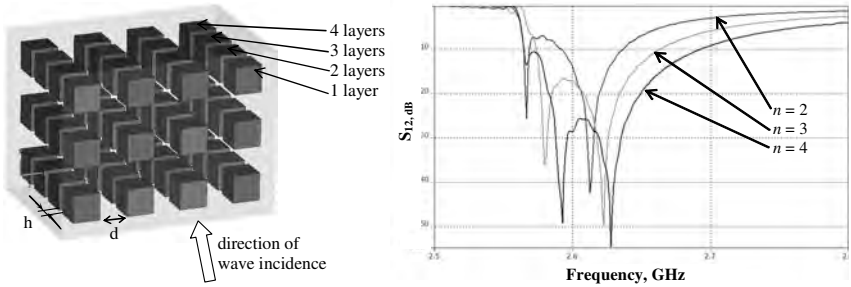


(a) (b)

Fig. 11. (a) Dielectric cubes structure with four cube layers. (b) Transmission coefficient for different number $n$ of layers, $d$ = 3 mm, $h$ = 1.2 mm.

The bi-cubic cell with dimensions: s = 3 mm, a = 1 mm, b = 1.36 mm and dielectric permittivity of the cubes $\varepsilon_{cub}$ = 60 and of the host material $\varepsilon_{host}$ = 1, was modelled. The transmission coefficient as a function of frequency is shown for the magnetic and dielectric resonances of single cube structures with the same resonant frequencies and for the bi-cubic structure as well. The pass band occurs at the resonant frequency for the bi-cubic structure (Fig. 12, (b)) confirming the metamaterial properties. The fields inside dielectric cubes in case of Mie resonances represent electric and magnetic dipoles (Fig 13).

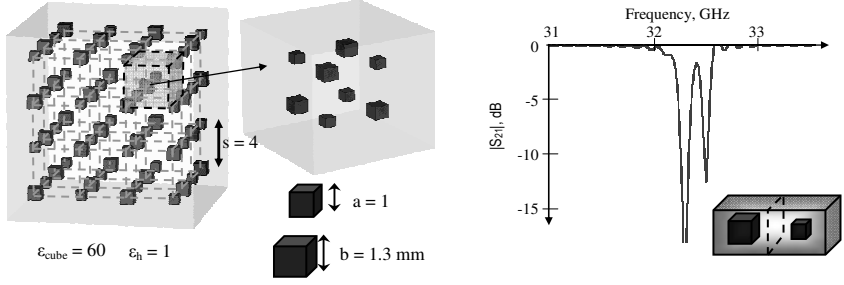


(a) (b)

Fig. 12. (a) Bi-cubic 3D structure of isotropic metamaterial; (b) pass band in the frequency region where first and second Mie-resonances coincide in small and large dielectric cubes.

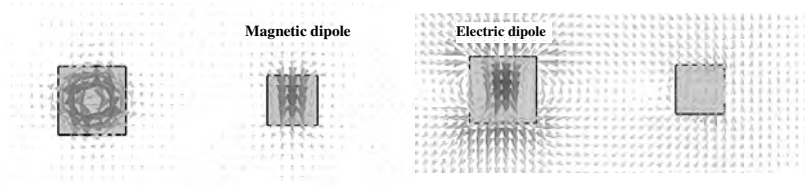


(a) (b)

Fig. 13. The electrical and magnetic field distribution for the first (a) and second (b) Mie resonances.



## 4. Low Limit for the Permittivity of Mie-Based Resonators in Homogeneous Metamaterials

An important problem is how to choose the parameters of the dielectric spherical resonators of the considered structure. Metamaterials can be considered as homogenous media described by effective permittivity and permeability under the condition that the period of the structure is much less than the wavelength of the electromagnetic wave propagating in the host material. As a criterion of homogeneity of the structure the following condition has been chosen: the maximum value of the structure period $s_{max}$ is equal to one quarter of the wavelength: [18]

$$s_{\max} = \lambda / 4 . \tag{4}$$

In case of $s < \lambda / 4$, the structure will be homogenous. At the same time the period of the structure has a lower bound, given by the physical size of the spherical resonators. Let us consider 3 possible structures with the cubic symmetry providing the isotropy of effective parameters (Fig. 1). Here $r_{small}$ and $r_{big}$ are the radii of small and large resonators respectively.

For all these structures $s_{\min} > 2(r_{small} + r_{big})$. Combining this condition with (4) we can describe the period by the following inequality:

$$2(r_{small} + r_{big}) < s < \lambda / 4 . \tag{5}$$

The radii of the resonators can be approximately defined as $r_{small} \approx \lambda_{sphere} / 2$ for magnetic resonance and $r_{big} \approx \frac{\lambda_{sphere}}{2} \frac{1}{0.7}$ for the electric resonance, where $\lambda_{sphere}$ is the wavelength inside the resonator. If radii of resonators are defined by these equations, two first Mie-

resonances (magnetic and electric) appear in the structure considered at the same frequency.

Inequality (5) can be rewritten in the following way:

$$\frac{2.41c}{f\sqrt{\varepsilon_{sphere}}} < s < \frac{c}{4f\sqrt{\varepsilon_h}}, \tag{6}$$

where $c$ is the light velocity, $f$ is the operating frequency, $\varepsilon_h$ and $\varepsilon_{sphere}$ are the host material and sphere permittivities respectively. Let us introduce the parameter $\delta_s$ which is determined as the difference between maximum and minimum values of the period:

$$\delta_s = \frac{c}{4f\sqrt{\varepsilon_h}} - \frac{2.41c}{f\sqrt{\varepsilon_{sphere}}}. \tag{7}$$

The dependence $\delta_s(\varepsilon_{sphere})$ for the isotropic metamaterial with host permittivity equal to unity is shown in Fig 14. All the curves on the graph intersect in one point, where $\varepsilon_{sphere}$ is equal to 100. The smaller values of $\delta_s$ parameter have no physical meaning.

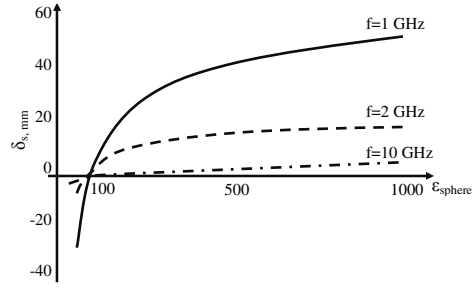


Fig. 14. Difference between maximum and minimum possible values of the period of structures depicted in Fig 1. The host permittivity is equal to vacuum permittivity.

All the structures depicted in Fig 1 can be realized by using resonators with permittivity $\varepsilon_{sphere} > 100$. It is important to note that the minimum value of the permittivity does not depend on the operating frequency. It depends only on the nature of electric and magnetic Mie-resonances in dielectric spherical particle and on the permittivity of the host material. If the permittivity of the host material becomes larger, the minimum possible value of $\varepsilon_{sphere}$ increases too.

The same limitations can be calculated for any other structure. As an example, consider the artificial magnetic material consisting of the dielectric spherical (or cubic) resonators of one kind, resonating on the first Mie resonance (Fig. 9). In this case, the minimum possible permittivity for the material of the spherical resonators should be 16. The same estimations could be made for rod, cylindrical resonators or any kind of dielectric resonators used as components for the metamaterial design.

## 5. DNG Metamaterial on the Regular Array of Strongly Coupled Spherical Resonant Inclusions

In the case the spacing between the adjacent dielectric spherical resonators is small, they start to interact. The coupling between the resonators leads to a change in the electromagnetic field distribution in the media outside the spheres. That makes it possible to get electric and magnetic dipole response: magnetic dipole comes from the first Mie resonance in the dielectric sphere, the electric dipole is formed by the sphere interaction conditioned by the electric field outside the sphere surface. Electric and magnetic dipole existence provides double negative response of the media.

1D regular structure of the spherical particles is shown in insets of Fig. 15. If the spacing is large enough, i.e. is larger than the sphere diameter, there is no interaction between the adjacent spheres. For the distantly positioned spheres the resonant stop-band is observed at the resonant frequency of the $TM_{111}$ mode (Fig. 15 a). By decreasing the spacing between the spheres, the splitting of the resonance characteristic occurs and the pass band appears near the resonant frequency (Fig 15 b). The electrical field distribution in the 1D structure of strongly coupled dielectric resonators is shown in Fig. 16.

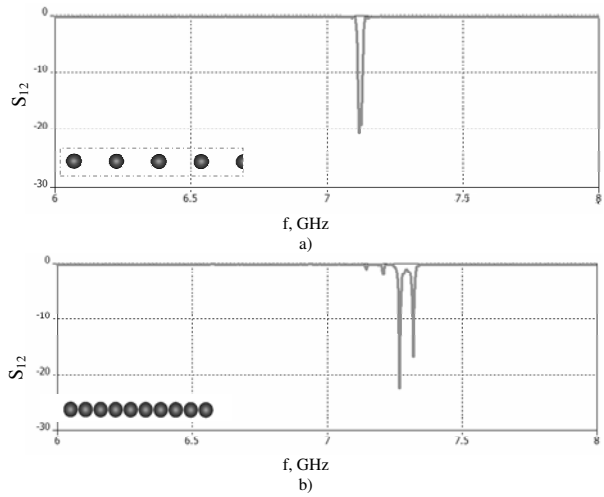


Fig. 15. Transmission coefficient of 1D structure distantly positioned non-coupled (a) and close positioned coupled (b) resonators.

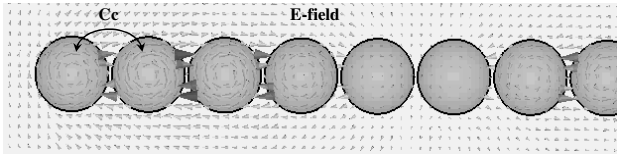


Fig 16. Electrical field between coupled resonators.

The one-dimensional case of the coupled resonant dielectric spheres can be considered as a dual analogue of the magneto-inductive waveguide [19, 20] described by an equivalent circuit of magnetically coupled series resonant tanks. In our case, the 1-D structure can be presented by electrically coupled parallel tanks.

As in the case of magneto-inductive waveguide, the stop-bands occur and the backward wave can be observed in the 1D-structure. The magnetic field distribution in the 1D-structure for different moments of the period of the electromagnetic wave demonstrates the backward wave propagation (Fig. 17). This result confirms the double negative properties of the structure.

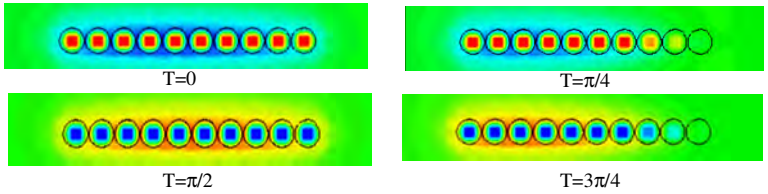


Fig. 17. The magnetic field distribution (y-component) in the 1D structure of coupled resonant spheres for different moments of the period of the wave.

A 2D plane structure consisting of 24 closely positioned dielectric spheres has been modelled. If the distance between the spheres is large, there is no wave propagation on a resonant frequency (Fig. 18 a). By

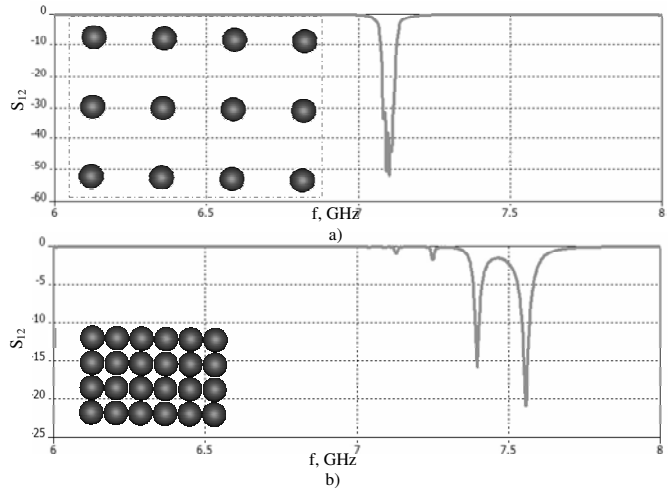


Fig. 18. Transmission coefficient of 2D structure distantly positioned non-coupled (a) and close positioned coupled (b) resonators.

decreasing the spacing between the spheres, the splitting of the resonance curve occurs (Fig. 18 b), and a pass band appears near the resonant frequency. Fig. 19 represents the phase diagram of the structure considered. The transverse magnetic field component in the free space is shown at the left side of the picture. The right side represents magnetic field pattern for the structure containing the regular array of the dielectric spheres. It is clearly seen from the magnified part of the picture that the phase response of the propagated electromagnetic wave inside the array of the spheres is positive, whereas the phase response outside the

structure is negative. This means there is a backward wave propagation in the structure considered.

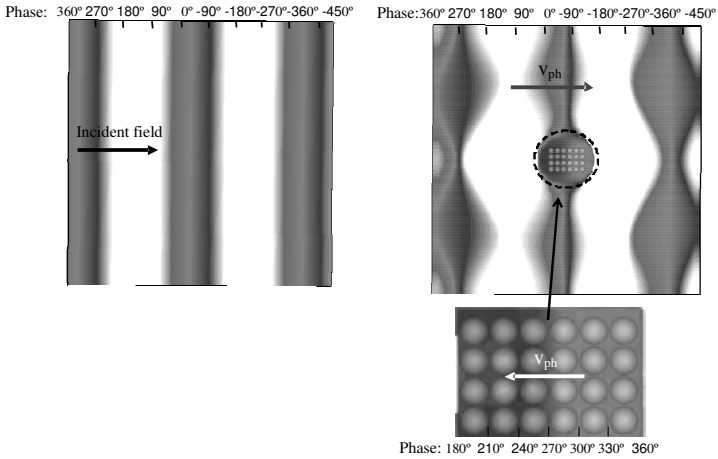


Fig. 19. Phase diagram of the 2D structure.

## 6. Conclusion

A double negative artificial material based on bi-spherical dielectric spherical and bi-cubic resonators has been investigated. In the case of distantly positioned particles when the interaction between particles can be neglected, and the system behaves as a homogeneous one for the incident wave, the isotropy of the structure is expected. The limitation of the dielectric properties of the resonant inclusions for the homogeneous 3D metamaterial is analyzed. The lower value of the dielectric permittivity is estimated.

A new structure with a higher packing density has been introduced in order to strengthen the DNG effect. Backward wave existence in the new structure has been confirmed by the numerical analysis. A concept of the metamaterial based on electrically coupled dielectric resonators was considered. Simulation results revealed the DNG behavior in 1D and 2D structures based on coupled dielectric resonators.

## References


1. C. Holloway and E. Kuester, *IEEE Trans. Antennas Propagat.* **51**, 2596 (2003).
2. O. G. Vendik and M. S. Gashinova, Proc. European Microwave Conference EuMC34, Paris, France, 2004, p. 1209.
3. I. Vendik, O. Vendik, and M. Gashinova, *Tech. Phys. Lett.* **32**, 429 (2006).
4. I. Vendik, O. Vendik, I. Kolmakov, and M. Odit. *Opto-Electronics Review* **14**, 179 (2006) .
5. M. Odit, I. Vendik, and O. Vendik, Proc. of Metamaterials 2007, Rome, Italy, 2007, p. 946.
6. A. Ahmadi and H. Mosallaei, .*Phys. Rev. B* **77**, 045104 (2008) .
7. T. Ueda, A. Lail, and T. Itoh, Proc. European Microwave Conference, EuMC36, 2005, p. 435.
8. E. A. Semouchkina, G. B. Semouchkin, M. Lanagan, and C. A. Randall, *IEEE Trans. Microwave Theory Tech.* **53**, 1477 (2005).
9. Q. Zhao, L. Kang, B. Du, H. Zhao, Q. Xie, X. Huang, B. Li, J. Zhou, and L. Li, *Phys. Rev. Lett.* **101**, 027402 (2008).
10. K. Shibuya, K. Takano, N. Matsumoto, K. Izumi, H. Miyazaki, Y. Jimba, and M. Hangyo, Proc. Metamaterial 2008, Pamplona, Spain, 2008, p. 777.
11. X. Cai, R. Zhu, and G. Hu, *Metamaterials* **2**, 220 (2008).
12. I. Vendik, M. Odit, and D. Kozlov, *Radioengineering* **18**(2), 111 (2009)
13. I. Vendik, O.G. Vendik, and M. Odit, Chap. 21 in *Theory and Phenomena of Metamaterials, Metamaterial Handbook*, Ed. F. Capolino (CRC Press, Taylor & Francis Group, 2009).
14. I.B. Vendik, M.A. Odit, and D.S. Kozlov, *Metamaterials* **3**, 140 (2009).
15. J.F. Nye, *Physical Properties of Crystals* (Clarendon Press, 1964).
16. E.A. Nenasheva, N.F. Kartenko, O.N. Trubitsina, V.F. Matveichuk, S.N. Sibirtsev, and I.M. Gaidamaka, *J. European Ceramic Soc.* **27**, 2845 (2007).
17. I.B. Vendik, O.G. Vendik, and M.A. Odit, *Phys. Solid States* **51**, 1590 (2009).
18. C. Caloz and T. Itoh, *Electromagnetic metamaterials: transmission line theory and microwave applications. The Engineering Approach* (John Wiley & Sons, Inc., Hoboken, 2006).
19. E. Shamonina, V. A. Kalinin, K. H. Ringhofer, and L. Solymar, *Electron. Lett.* **38**, 371 (2002).
20. E. Shamonina, V. A. Kalinin, K. H. Ringhofer, and L. Solymar, *J. Appl. Phys.* **92**, 6252 (2002).